COMMUNICATION

ChemComm
www.rsc.org/chemcomm

Metal organic chemical vapour deposition (MOCVD) of bone mineral like carbonated hydroxyapatite coatings†

J. A. Darr,*[a] Z. X. Guo,[a] V. Raman,[a] M. Bououdina[a] and I. U. Rehman[b]
[a] *Department of Materials, Queen Mary University of London (QMUL), Mile End Road, London, UK E1 4NS. E-mail: j.a.darr@qmul.ac.uk; x.guo@qmul.ac.uk*
[b] *Interdisciplinary Research Centre in Biomedical Materials, QMUL, Mile End Road, London, UK E1 4NS. E-mail: i.u.rehman@qmul.ac.uk*

Received (in Cambridge, UK) 14th October 2003, Accepted 21st January 2004
First published as an Advance Article on the web 13th February 2004

For the first time, the MOCVD technique has been used to deposit carbonated hydroxyapatite onto Ti6AL4V substrates using volatile monomeric (liquid) complexes [Ca(β-diketonate)$_2$(L)] and P(OEt)$_3$.

Metal organic chemical vapour deposition (MOCVD) has been widely used to prepare coatings in the semiconductor industry and has shown several benefits compared with other coating methods.[1,2] The key advantages of this technique include the ability to modulate precursor concentrations during deposition to create functionally graded coatings (FGC).[2] Bioactive surface coatings are becoming of increased importance for the development of more biocompatible implants and biosensors. Calcium phosphate (CAP) based coatings such as hydroxyapatite (HA) [$(Ca_{10}(PO_4)_6(OH)_2)$], have been given much attention recently due their biocompatible and bioactive properties and ability to bond to host tissues.[3] The Ca:P ratio of calcium phosphates and the substitution of ions into the structure such as carbonate, fluoride, silicate, *etc*., can greatly improve resorbability, bioactivity and osteoconduction.[4,5,6] Several methods have been used to coat bioceramics onto implants including plasma spraying,[7] pulsed laser deposition,[8] ion beam sputtering,[9] electrodeposition[10] and RF magnetron sputtering.[11] In many cases, the coatings can only be formed with a specific composition and problems are encountered such as poor adhesion of coatings onto the substrate. In a previous study, Ciliberto and co-workers used the polymeric solids, $[Ca(tmhd)_2]_\infty$ (where tmhd = 2,2,6,6,-tetramethylheptane-3,5-dione) and $[P_2O_5]_\infty$, respectively, to deposit a calcium phosphate on an alumina substrate.[12] Since this study, there have been significant developments in the field of volatile calcium precursors suitable for CVD. In particular, complexes with the formula [Ca(β-diket)$_2$(L)] (where β-diket = tmhd,[13] 1,1,1,2,2,3,3,7,7,8,8,9,9,9,-tetradecafluorononane-4,6-dionate (tdfnd),[14] 1,1,1,2,2,3,3,7,7,7,-decafluoroheptane-2,4-dionate (tdfhd)[15] and L = monoglyme, diglyme, triglyme, tetraglyme, heptaglyme[16]], can be made with high purity and exhibit excellent evaporation (sublimation) behaviour. Due to their low melting points, these compounds are used as liquids in the CVD bubbler system as they exhibit higher vapour pressures and more uniform carry over rates compared with solids.

The first MOCVD deposition of a fluorine-containing carbonated hydroxyapatite (CHA) coating using *only volatile metal-organic precursors* is reported herein. The coating was deposited in a custom-built MOCVD apparatus using argon carrier gas in the bubblers and precursors of [Ca(hfpd)$_2$(tetraglyme)] (CAT) (where hfpd = 1,1,1,5,5,5,-hexafluro-2,4-pentadione) and tributylphosphate (TBP), respectively.‡ Deposition on 20 × 5 mm (125 μm thick) Ti6Al4V metal plates was conducted at *ca.* 600 °C. The cooled substrate was then taken from the chamber and then one half of the sample was sintered in air at 800 °C for 3 hours prior to analyses. Fig. 1 shows a scanning electron microscope (SEM) image of the 'as deposited' and sintered coating on the plate surface. The 'as deposited' coating is characterised by cauliflower-like nodules which have grown over the entire surface area of the substrate. The average nodule size was found to range between 5–8 μm (Fig. 1a). This suggests that CAP crystals are seeded on the surface or gas phase and agglomeration of primary nuclei occurs. At higher magnification under the SEM (×1000), the cauliflower nodules are shown to be made of tightly packed particles that form agglomerates of *ca.* 1 μm or smaller (Fig. 1b).

EDX analysis of the unsintered coating suggests a calcium/phosphate ratio, Ca/P of 1.3. Fig. 1b shows the SEM image of the specimen after 3 hours sintering. The coating underwent significant shrinkage to form large agglomerates on the surface of the coating. The largest particles are now about 20–22 μm whilst the smaller particles average between 1–2 μm in diameter (Fig. 1c). The pillar structures noted in the unsintered images are no longer present and closer inspection under SEM revealed that the smaller particles have partially fused together (Fig. 1d). EDX analysis of the sintered film suggested a Ca/P ratio of 1.71. EDX analysis also suggested the presence of small quantities of fluorine in the coating.

FT-Raman and FTIR spectroscopy were performed on the sintered specimens. (Figs. 2 and 3, respectively). The Raman spectrum for our coating shows similarities to that for commercial hydroxyapatite and human bone mineral, respectively. Phosphate

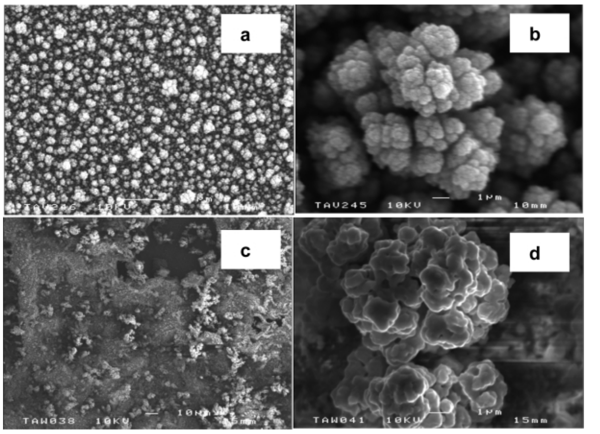

Fig. 1 As deposited coating at (a) low magnification, (b) ×1000 magnification and sintered coating at (c) low magnification, (d) ×1000 magnification.

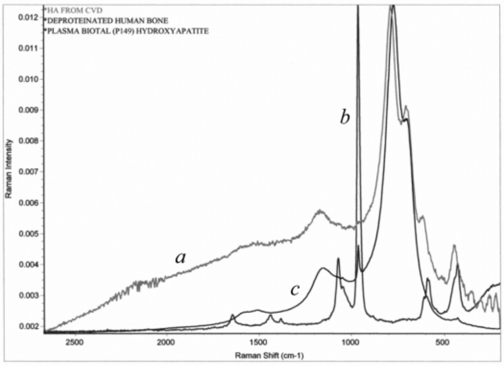

Fig. 2 Raman spectrum for (*a*) sintered CVD coating, (*b*) deproteinated human bone mineral and (*c*) commercial HA (Plasma Biotol P120).

---

† Electronic supplementary information (ESI) available: experimental data. See http://www.rsc.org/suppdata/cc/b3/b312855p/

DOI: 10.1039/b312855p

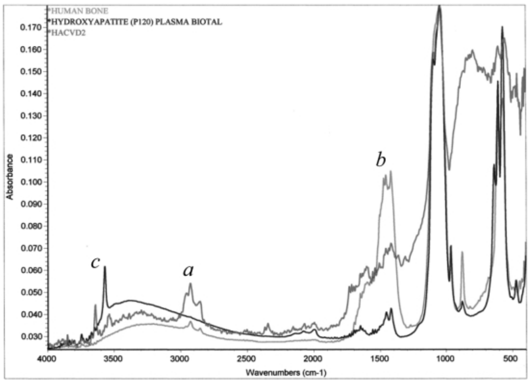

Fig. 3 FTIR spectrum of (*a*) sintered CVD coating, (*b*) deproteinated human bone mineral and (*c*) commercial HA (Plasma Biotol P120).

peaks observed in the region 953–444 cm^{-1} were clearly defined and identified; a symmetric phosphate stretch at 953 cm^{-1}, an asymmetric phosphate stretch at 786 cm^{-1} and phosphate bends at 702 cm^{-1} and 444 cm^{-1}, respectively. In comparison, the Raman spectrum of synthetic hydroxyapatite (reported by Rehman *et al.*)[18] shows peaks at 952, 774, and 436 cm^{-1}, respectively. The Raman spectrum of our coating also revealed a peak at 610 cm^{-1}, which is due to the metal oxide (M-O stretches) of the substrate. The FTIR spectrum of the coating revealed sharp peaks due to phosphate bends at 1096 and 1044 cm^{-1} (υ_3), and 605 and 566 cm^{-1} (υ_4), respectively. A further peak at 982 cm^{-1} suggested the presence of a phosphate symmetric stretch (υ_1). These peaks are comparable to the FTIR spectral data reported by Rehman *et al.*[19] on bone, HA and calcium apatite in which phosphate bends were observed at 1040 cm^{-1} (υ_3) and 629, 603 and 567 cm^{-1} (all three υ_4), respectively, and a phosphate symmetric stretch (υ_1) was observed at 961 cm^{-1}

Tadic *et al*. reported that the characteristic splitting of the peaks at phosphate bend (υ_3) and asymmetric stretch (υ_2) peaks indicates a degree of crystallinity within the specimen.[20] A similar observation was made in our coating. The presence of carbonate is suggested by the peaks at 1417 and 860 cm^{-1}, which are associated with the CO_3 (υ_3) and (υ_2) vibrational modes, respectively. These peaks are comparable to the reference spectrum of bone that shows carbonate bending (υ_3) and asymmetric stretching (υ_2) peaks at 1417 and 873 cm^{-1}, respectively. The FTIR spectrum of the coating also revealed a peak at 3538 cm^{-1} and peaks between 2947–2853 cm^{-1}, which are likely to be due to hydroxy and C–H stretches, respectively. The C–H bands could be due to organic residues, which have not been completely removed as a result of mild sintering. By changing the heating conditions or through possible addition of additional gases such as moist air, it may be possible to reduce or eliminate such impurities. The deposition of carbonated calcium hydroxyapatite *via* the MOCVD method represents a new method for producing bioceramic coatings from liquid or volatile molecular precursors.

The coating has a cauliflower-like agglomerated structure and composition with some similarities to human bone mineral. The coating also contains fluorine impurity, which could ultimately improve the biocompatibility of the coating. The MOCVD process has potential to add other beneficial dopants, *e.g.* Na, Mg or F by addition of co-reagents in the gas phase to produce coatings with specific biological properties. Further studies are currently underway into introducing such elements and evaluating their biological properties.

The authors wish to thank the EPSRC for funding and for an EPSRC Advanced Research fellowship (JAD) and core IRC funding (IR). We also thank John Caulfield, Zofia Luklinska, Monisha Phillips and Vince Ford for technical assistance.

Notes and references

‡ Simultaneous thermal analysis (STA) data for CAT revealed that the compound melted at 120 °C and sublimed intact between 170–300 °C to give 99% loss of initial mass. However, in the bubbler, it sublimed at a lower temperature of 125 °C. The TGA plot for the phosphate precursor showed complete sublimation between 125–190°C.

The custom-built MOCVD apparatus consists of three major sections; (i) a precursor delivery and mixing system (ii) a deposition chamber, and (iii) an exhaust outlet. The deposition chamber was a cold wall-reactor system and the supply carrier gas used was Argon. TBP was used as obtained (Aldrich Chemical Co.) and CAT was synthesized in house from calcium carbonate (Aldrich Chemical) and HFPD (Fisher Scientific Chemicals) using a modified method to that reported for similar compounds.[17] For each experiment, commercially available 125 μm thick Ti6Al4V metal plates (Advent Research Materials) were fastened to tungsten electrodes and then heated to 600 °C by resistant heating. The temperature was calculated by comparing the colour of the glow against a metallographic colour chart. 30 ml of CAT and TBP, respectively, were placed in the respective bubblers and heated to 125 °C using two 450 Watt electromantles. Prior to operating the reactor, the deposition chamber was flooded with argon to create a non-oxidative environment. The outer-rig was kept at 130 °C to prevent condensation of precursors. The flow rates were fixed at 16.6 ml s^{-1} for CAT and 12.5 ml s^{-1} for TBP, respectively. The vaporised precursors were forced through a flow mixer to encourage blending. The coatings were analysed under a JEOL 6300 SEM with INCA Energy 300 Microanalysis EDS system. Sintered specimens were analysed on a Raman spectrometer (Nicolet 910 spectrophotometer equipped with an Nd:YVO_4 near-infrared laser) and a FTIR spectrometer (Nicolet 800 spectrometer employing a MTech Photoacoustic (PAS) cell for sampling).

1 K. L. Choy, *Prog. Mater. Sci.*, 2003, **48**, 63.
2 H. O. Pierson, *Handbook of chemical vapor deposition (CVD): principles, technology, and applications*, Noyes Pub., 1992.
3 H. Aoki, *Science and medical applications of hydroxyapatite*, Takayama Press System Center, 1991, 165.
4 H. W. Denissen, *Dutch Soc. Electron Microsc.*, 1980, **4**, 124.
5 R. Murugan, T. S. S. Kumar and K. P. Rao, *Mater. Lett.*, 2002, **57**, 429.
6 F. Monchau, A. Lefe'vre, M. Descamps, A. Belquin-Myrdycz, P. Laffargue and H. F. Hildebrand, *Biomol. Eng.*, 2002, **19**, 143.
7 K. A. Gross, *J. Mater. Sci. Mater. Med.*, 1994, **5**, 219.
8 J. M. Fernández-Pradas, L. Clèries, G. Sardin and J. L. Morenza, *Biomaterials*, 2002, **23**, 1989.
9 M. Manso, C. Jiménez, C. Morant, P. Herrero and J. M. Martínez-Duart, *Biomaterials*, 2000, **21**, 1755.
10 J. Choi, H. Kim and I. Lee, *Biomaterials*, 2000, **21**, 469.
11 J. D. Long, S. Xu, J. W. Cai, N. Jiang, J. H. Lu, K. N. Ostrikov and C. H. Diong, *Mat. Sci. Eng.*, 2002, **20**, 175.
12 G. C. Allen, E. Ciliberto, I. Fragala and G. Spoto, *Nucl. Instrum. Methods Phys. Res. B*, 1996, **116**, 457.
13 S. H. Shamilian, M. L. Hitchman, S. L. Cook and B. C. Richards, *J. Mater. Chem.*, 1994, **4**, 81.
14 S. C. Thompson, D. J. Cole-Hamilton, D. D. Gilliland, M. L. Hitchman and J. C. Barnes, *Adv. Mater. Opt. Electron.*, 1992, **1**, 81.
15 I. Baxter, S. R. Drake, M. B. Hursthouse, K. M. Abdul Malik, J. McAleese, D. J. Otway and J. C. Plakatouras, *Inorg. Chem.*, 1995, **34**, 1384.
16 S. R. Drake, M. B. Hursthouse, K. M. Abdul Malik and S. A. S. Miller, *Inorg. Chem.*, 1993, **32**, 1970.
17 V.-C. Arunasalam, I. Baxter, S. R. Drake, M. B. Hursthouse, K. M. Abdul Malik, S. A. S. Miller, D. M. P. Mingos and D. J. Otway, *J. Chem. Soc., Dalton Trans.*, 1997, **8**, 1331.
18 I. Rehman, R. Smith, L. L. Hench and W. Bonfield, *J. Biomed. Mater. Res.*, 1995, **29**, 1297.
19 I. Rehman and W. Bonfield, *J. Mater. Sci.; Mater. Med.*, 1997, **8**, 1–4.
20 D. Tadic, F. Peters and M. Epple, *Biomaterials*, 2002, **23**, 2553.